The Plant Cell, Vol. 12, 853–870, June 2000, www.plantcell.org © 2000 American Society of Plant Physiologists

STEROL METHYLTRANSFERASE 1 Controls the Level of Cholesterol in Plants

Andrew C. Diener,[a] Haoxia Li,[b] Wen-xu Zhou,[b] Wendy J. Whoriskey,[c] W. David Nes,[b] and Gerald R. Fink[a,1]

[a] Whitehead Institute for Biomedical Research, and Department of Biology, Massachusetts Institute of Technology, Cambridge, Massachusetts 02142

[b] Department of Chemistry and Biochemistry, Texas Tech University, Lubbock, Texas 79409

[c] Dana-Farber Cancer Institute, and Department of Pathology, Harvard Medical School, Boston, Massachusetts 02115

The side chain in plant sterols can have either a methyl or ethyl addition at carbon 24 that is absent in cholesterol. The ethyl addition is the product of two sequential methyl additions. Arabidopsis contains three genes—*sterol methyltransferase 1* (*SMT1*), *SMT2*, and *SMT3*—homologous to yeast *ERG6*, which is known to encode an *S*-adenosylmethionine–dependent C-24 SMT that catalyzes a single methyl addition. The SMT1 polypeptide is the most similar of these Arabidopsis homologs to yeast Erg6p. Moreover, expression of Arabidopsis *SMT1* in *erg6* restores SMT activity to the yeast mutant. The *smt1* plants have pleiotropic defects: poor growth and fertility, sensitivity of the root to calcium, and a loss of proper embryo morphogenesis. *smt1* has an altered sterol content: it accumulates cholesterol and has less C-24 alkylated sterols content. *Escherichia coli* extracts, obtained from a strain expressing the Arabidopsis SMT1 protein, can perform both the methyl and ethyl additions to appropriate sterol substrates, although with different kinetics. The fact that *smt1* null mutants still produce alkylated sterols and that SMT1 can catalyze both alkylation steps shows that there is considerable overlap in the substrate specificity of enzymes in sterol biosynthesis. The availability of the *SMT1* gene and mutant should permit the manipulation of phytosterol composition, which will help elucidate the role of sterols in animal nutrition.

INTRODUCTION

Sterols are ubiquitous among eukaryotic organisms and serve both as bulk membrane lipid components and as precursors for additional metabolites such as mammalian steroid hormones, plant brassinosteroid hormones, and insect ecdysteroids (Parish and Nes, 1997).

The major sterols of plants and fungi contain an alkyl substitution at carbon 24 that is absent in cholesterol, the dominant sterol of virtually all animals (Nes and McKean, 1977). The methyl and ethyl substituents at C-24 are the only sterol carbons not derived from the acetate–mevalonate pathway and are absent in the first sterol intermediate of plants (cycloartenol) as well as animals and fungi (lanosterol) (Nes and McKean, 1977).

The carbons of the alkyl group at C-24 are added by way of an *S*-adenosylmethionine (SAM)–dependent transmethylation (Parks, 1958). The methyl (C_1) or ethyl (C_2) substituent at C-24 is the product of either a single carbon addition or two sequential single carbon additions. The alkylation product of the first transmethylation, a C-24 methylene (C_1) sterol, is the substrate for the second transmethylation reaction to generate a C-24 ethylidene (C_2) sterol (Castle et al., 1963).

The first and second C-methyl additions are performed as distinct steps in phytosterol synthesis (Figure 1) by the enzyme SMT. However, the C-24 SMT, like other enzymes in sterol biosynthesis, can be somewhat promiscuous. In photosynthetic organisms, cycloartenol is thought to be the substrate of the first methylation (Figure 1, step 1) because 24-methylene cycloartenol, the earliest possible product of transmethylation, is a frequently detected minor (and presumably intermediate) sterol in plant extracts (Guo et al., 1995). Moreover, cycloartenol is the best in vitro substrate for C-24 methyl addition, compared with other potential sterol intermediates (Nes et al., 1991, 1998b). 24-Methylene lophenol is often considered the optimal substrate for the second transmethylation (Figure 1, step 7) (Rahier et al., 1986).

In the fungus *Saccharomyces cerevisiae*, the transmethylation that produces the dominant 24-methyl sterol, ergosterol, is performed by a SAM-dependent C-24 SMT, Erg6p (Bard, 1972). The *erg6* mutant, isolated for its resistance to the polyene antibiotic nystatin, was the first recognized yeast mutant with a deficiency in ergosterol biosynthesis

[1] To whom correspondence should be addressed at Whitehead Institute for Biomedical Research, 9 Cambridge Center, Cambridge, MA 02142-1479. E-mail fink@wi.mit.edu; fax 617-258-9872.

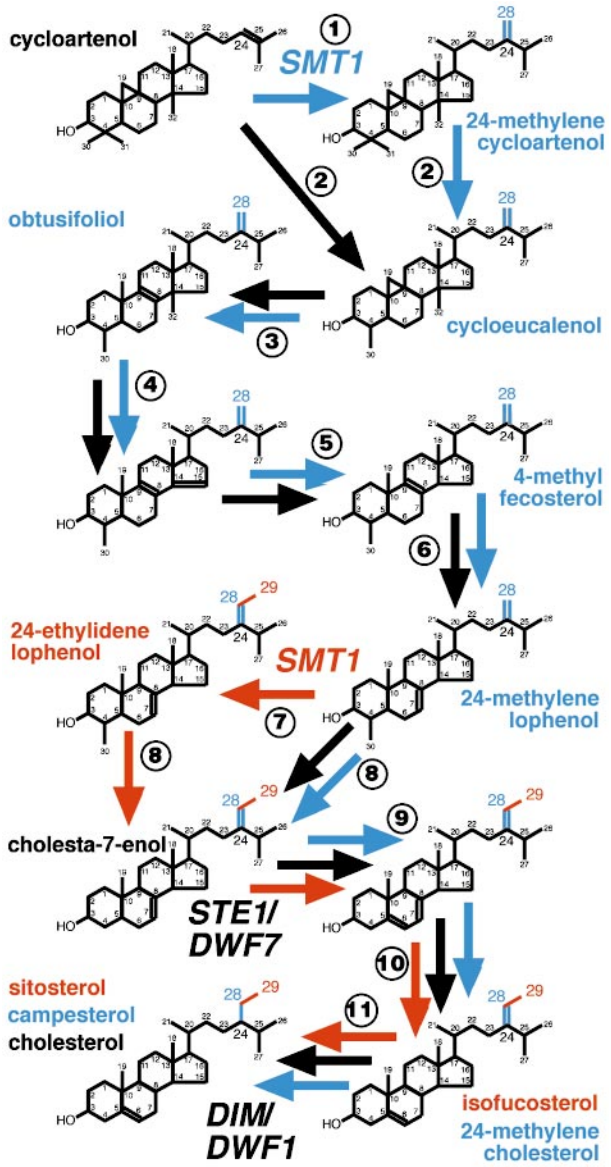

Figure 1. Phytosterol Biosynthetic Pathway.

Cycloartenol, the first polycyclic sterol intermediate, is converted into the dominant C5-sterols: cholesterol, campesterol, and sitosterol. The color code distinguishes the degree of C-24 alkylation (blue for the C_1 addition and red for the C_2 addition) on the black carbon skeleton of the sterol intermediates or products. For the names of the products and some intermediates, the color indicates whether the sterol has no addition (black), C_1 addition (blue), or C_2 addition (red) at C-24. The kinetically favored pathway for biosynthesis of cholesterol (black), campesterol (blue), and sitosterol (red) is also indicated with colored arrows. The enzymatic steps are numbered as follows: 1, *S*-adenosyl-L-methionine:C24(25) C-methyltransferase; 2, C-4 methyl oxidase/C-3 dehydrogenase/C-3 keto reductase; 3, cycloeucalenol-obtusifoliol isomerase; 4, C-14 demethylase; 5, C14 reductase; 6, C8-C7 isomerase; 7, *S*-adenosyl-L-methionine:C24(28) C-methyltransferase; 8, C-4 methyl oxidase/C-3 dehydrogenase/C-3 keto reductase; 9, C5 desaturase; 10, C7 reductase; and 11, C24(25) reductase.

(Molzahn and Woods, 1972). Mutants defective in late steps of sterol biosynthesis show reduced sensitivity to polyenes such as nystatin that disrupt the membranes, although the connection between nystatin resistance and the defect in ergosterol biosynthesis is not completely understood.

The *erg6* defect in ergosterol biosynthesis leads to a broad spectrum of phenotypes that can be attributed to a lack of membrane integrity. For example, *erg6* mutants are hypersensitive to hypertonic shock with various metal salts (Bard et al., 1978), hypersensitive to Na^+ and Li^+ (Welihinda et al., 1994), supersensitive to recovery from arrest by nalidixic acid (Prendergast et al., 1995), deficient in active tryptophan uptake (Gaber et al., 1989), and more readily absorbent of the dye crystal violet than is the wild type (Bard et al., 1978). Because the *erg6* mutation increases permeability, it is useful for studying small molecules such as brefeldin A that fail to enter wild-type cells efficiently (Shah and Klausner, 1993).

The SMTs from other fungi and plants have been identified by either their sequence similarity to yeast Erg6p or their ability to suppress defects of the yeast *erg6* mutant (Hardwick and Pelham, 1994; Husselstein et al., 1996; Shi et al., 1996; Jensen-Pergakes et al., 1998). The SMTs from diverse organisms are clearly related and fall into three classes, based on sequence relatedness: a distinct class of fungal genes and two classes of plant genes. The fungal *ERG6* genes from *S. cerevisiae*, *Candida albicans*, and *Schizosaccharomyces pombe* share at least 52% identity to each other and somewhat less (no more than 43% identity) to any of the plant SMT genes (Jensen-Pergakes et al., 1998). Members of the first class of plant SMTs are at least 69% identical to each other and no more than 47% identical to sequences in the two other classes. A second class of plant SMTs shares at least 71% identity among its members and has no more than 42% identity to members in the other two classes (Bouvier-Nave et al., 1998).

The two sequence-related classes of plant SMT proteins are thought to reflect their roles in distinct enzymatic steps (Grebenok et al., 1997; Bouvier-Nave et al., 1998). Because the first class shares more sequence conservation with the fungal *ERG6* genes (which exclusively produce methylated sterols, or C_1 addition) than does the second class, the first class of plant SMTs is proposed to be responsible, in planta, for the first SMT step. The members of the second class of plant SMTs, which are more distantly related to *ERG6*, are proposed to perform in planta the second SMT step responsible for C_2 substitution (Husselstein et al., 1996; Bouvier-Nave et al., 1998). The available set of plant SMT sequences discounts a phylogenetic significance for the two classes

because the genomes of both monocot and dicot plants contain members of both SMT groups.

Despite this categorization, recent biochemical analysis of plant SMT activities indicates that the functional distinction may not be so clearly defined (Bouvier-Nave et al., 1998). Members from either SMT class are capable of performing both C_1 and C_2 additions but can differ with respect to substrate affinities, substrate reaction rates, or allosteric modulation. Heterologous expression of either class one or class two enzymes from tobacco (Ntsmt1-1 or Ntsmt2-1) in the *erg6* yeast mutant leads to the accumulation of both C_1 (ergosterol) and C_2 (24-ethylidene-24,25-dihydrolanosterol) alkylated sterols, whereas the *erg6* mutant alone accumulates only sterols lacking the C-24 methyl group (Bouvier-Nave et al., 1998).

The Arabidopsis genome contains at least three genes related to *ERG6*. Two of the genes, *SMT2* and *SMT3*, have been cloned and expressed in yeast. Each is capable of promoting both C_1 and C_2 addition when expressed in *erg6* yeast cells (Bouvier-Nave et al., 1997; Schaller et al., 1998). Also, SMT2 can perform both C-methyl additions stereoselectively when expressed in *Escherichia coli* (Tong et al., 1997). These data suggest that the plant enzymes are ordinarily capable of both the C_1 and C_2 additions.

In this report we identify the function of the third Arabidopsis SMT gene *SMT1* by the expression of the cloned gene and the analysis of mutants lacking this enzyme. Until now, the functional importance for the C-24 alkylation of sterols in plants has been appraised only indirectly (Bloch, 1983; Hartmann, 1998). Here, we describe the phenotypic defects associated with the diminished sterol C-24 alkylation resulting from the absence of the Arabidopsis class one C-24 SMT.

RESULTS

smt1 Mutant

A screen of *Ac*-mutagenized seed pools for plants displaying abnormal root system formation yielded four independent strains with very similar root growth defects (James et al., 1995). All four mutants were also indistinguishable with respect to the other phenotypes we observed. Subsequent analysis showed that all four mutations are in a gene encoding an SMT. The mutants, as shown in Figure 2, have shorter petioles and smaller, rounder leaves, which make their rosettes more compact than that of the wild-type *SMT1* plant; moreover, the stems of *smt1* plants are shorter than those of *SMT1*. Although the *smt1* flowers appear normal, the siliques that develop are stunted.

Two of the alleles, *smt1-2* and *smt1-3,* were shown to segregate as single, recessive Mendelian traits (Table 1). Crosses of either *smt1-2* or *smt1-3* to wild-type Wassilewskija (Ws) or Columbia ecotype, respectively, yielded 18% F_2 progeny with the mutant phenotype of the original *smt1* parent. The lower than expected frequencies of Smt^- plants in one of the crosses may be attributable to a selective disadvantage of the *smt1* gametes.

Figure 2. Comparison of *smt1*and *SMT1* Plants.

(A) Rosette of 2-week-old *SMT1*/*SMT1* plant.
(B) Rosette of 2-week-old *smt1-3*/*smt1-3* plant.
(C) Mature (5-week-old) *SMT1* and *smt1-3* plants.

Table 1. *smt1* Is a Recessive Mutation

Cross[a]	F_2 Smt$^+$	F_2 Smt$^-$	P[b]
smt1-2 (Ws) × *SMT1* (Ws)	195	43	$P > 0.1$
smt1-3 (Ws) × *SMT1* (Col)	454	101	$P < 0.005$

[a] The parental genotype (and ecotype background). Col, Columbia.
[b] Probability, derived from chi square test, that the observed segregation results from the 3 (Smt$^+$):1 (Smt$^-$) ratio expected for a recessive mutation.

Conditional *smt1* Root Growth

The *smt1* mutants were initially identified on agar plates for their stunted and disfigured roots with swelling in the epidermis and cortex, as seen in Figure 3. In the figure, the meristems of the more severely distorted roots are arrested. In the differentiation zone, in which wild-type root cells in the cortex and epidermis are rectangular and elongated, the same cells in *smt1* roots are rounded and stunted (Figures 3F and 3G). Along the root length, the cell files in the *smt1* root lack their characteristic order and delineation, which may be responsible for the disordered pattern of root hair growth on the epidermis.

Surprisingly, *smt1* plants grown in soil had normal-looking roots that were indistinguishable from the roots of wild-type *SMT1* plants. The aberrant root phenotype on agar medium was not accentuated or rescued by changing various growth parameters (see Methods). However, after ~2 weeks of growth, the roots of *smt1-3* plants shown in Figure 3D are indistinguishable from those of the wild type shown in Figure 3C. One explanation for this behavior is that some component of the agar medium that is inhibitory to the roots of *smt1* seedlings is detoxified over time so that the *smt1* roots can expand normally.

A test of the various components of the plant nutrient agar growth medium (PNG; see Methods for composition) revealed that the *smt1-1* strains were sensitive to the calcium salt concentration. Decreasing the plant nutrient salt concentration by 10-fold led to marked improvement in the growth of *smt1-1* and *smt1-3* roots, whereas alteration of other medium components had no effect. To identify the inhibitory ion or ions, we tested the growth of the mutant on PNG in which each component salt (see Methods) was diluted 10-fold. Decreasing the calcium salt gave a noticeable improvement in root growth: a longer primary root and improved overall appearance. The same change in calcium salt concentration had no effect on wild-type roots. Because this sensitivity was apparent with medium containing either $CaCl_2$ or $Ca(NO_3)_2$, we conclude that the mutant is hypersensitive to calcium ions. The fact that the mutant phenotype could not be completely suppressed by lowering the calcium concentration suggests that other inhibitory factors are also present in the agar medium.

smt1 Plants Have Low Fertility

smt1 plants produce normal flowers but have severely reduced fertility, yielding at most one to two viable seeds per silique. The drastic reduction in fertility results from aborted embryos, not reduced fertilization. The pollen produced by *smt1* plants covers the stigmas of these *smt1* plants. Moreover, microscopic inspection of the *smt1* pollen tubes indi-

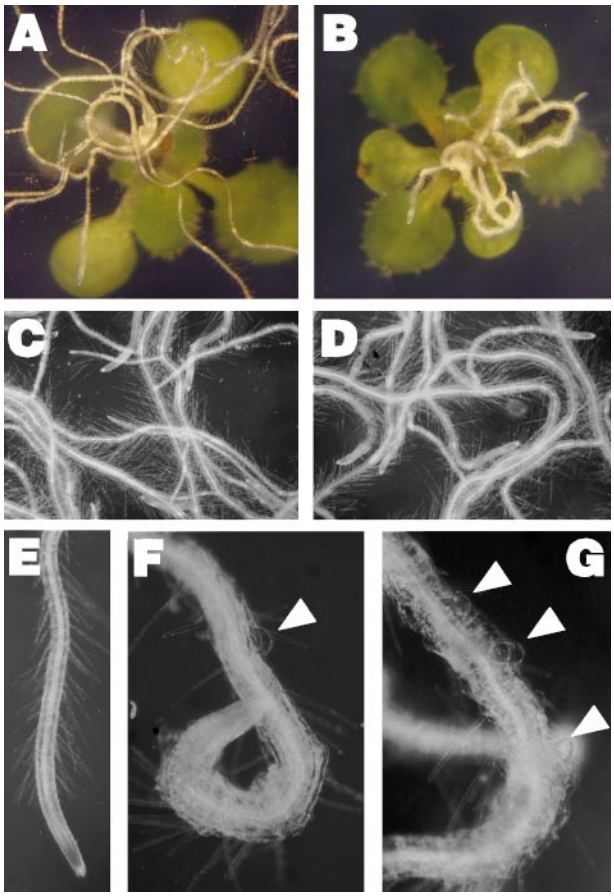

Figure 3. *smt1* Root Growth.

(A) and **(B)** As seen upside down from the bottom of an agar plate, the roots of wild-type *SMT1* **(A)** and *smt1-3* **(B)** grown for 1.5 weeks on PNG plates.
(C) and **(D)** Higher magnification of the same plates as in **(A)** and **(B)**, respectively, now ~5 weeks old.
(E) The primary root of the wild type.
(F) and **(G)** The swollen *smt1* primary root grown on agar plates. The white triangles point to abnormal swelling of root epidermal cells.

cates that these tubes appear to grow into the stigma and to the ovules in a manner indistinguishable from wild-type pollen tubes. In addition, in *smt1* plants with good overall growth, most ovules are fertilized. Inspection of immature siliques, cleared and dissected, revealed that 85% of ovaries from *smt1* plants—412 ovaries from 16 siliques were examined—contained developing embryos, whereas in self-fertilized wild-type plants, 94% of all ovaries—374 ovaries from eight siliques were examined—contained developing embryos. This slight difference in fertilization does not explain the much lower seed yield of *smt1* plants.

Rather, most embryos of *smt1* abort. From the appearance of dissected seeds, the abortion does not seem to occur at a particular developmental stage. At early stages of embryogenesis, regions of the normally colorless embryo sac may appear darkened and presumably necrotic, usually including regions closest to the funicle attachment, the chalazal nucellus, as seen in Figures 4G and 4I to 4M.

The infertility caused by *smt1* appears to be a recessive maternal defect. The *SMT1*/*smt1* heterozygote is completely fertile and produces nearly a quarter *smt1*/*smt1* viable seeds. Moreover, crosses in which pollen from an *smt1*/*smt1* plant is crossed onto an *SMT1*/*SMT1* stigma are fertile; however, repeated attempts to make the reciprocal cross by placing *SMT1* pollen onto *smt1*/*smt1* stigmas failed to produce any seed.

smt1 Embryogenesis Is Aberrant

Of those few seeds obtained from self-fertilized *smt1* plants, roughly three-quarters germinated on agar plates. However, the embryos formed in the germinated seedlings revealed various defects. The most remarkable feature of the *smt1* seedlings is the variable number and shape of their cotyledons. Representative seedlings with aberrant cotyledon structures are shown in Figures 4P and 4Q, along with the usual dicot seedling for comparison.

To examine this defective embryogenesis, we compared the developing embryos from the wild type shown in Figures 4A to 4E and *smt1-3* plants shown in Figures 4F to 4J. The *smt1* embryos from all four *smt1* alleles have difficulty forming the gross structures that distinguish the different stages of embryogenesis, for example, the projections in the heart stage or torpedo stage that give rise to the cotyledons. In comparison with the wild type, the cell mass in an *smt1* embryo has a flattened or dulled shape.

Observations suggest that the aberrant shape of the *smt1*/*smt1* embryos is not a maternal defect. The 18% *smt1*/*smt1* progeny obtained from self-fertilized *SMT1*/*smt1* heterozygotes frequently possess an aberrant number of cotyledons and a shape similar to the *smt1*/*smt1* progeny of self-fertilized *smt1*/*smt1* homozygotes. As described below, the expression of a transgenic *SMT1* cDNA partially complemented *smt1-3*, restoring fertility but not normal embryo morphogenesis. This dichotomy suggests that these two phenotypes are the outcomes of two distinct processes.

In addition, *smt1* seedlings have an apparent requirement for an exogenous carbon energy source such as glucose or sucrose after germination (as described in Methods). The amounts of major seed storage proteins and triacylglycerols contained in *smt1-1* and *smt1-3* seeds are comparable with those of the wild type (A.C. Diener, unpublished results), making it unlikely that diminished stores of these compounds are the basis of the carbon source requirement.

smt1 Mutants Are the Result of DNA Rearrangements

Two of the four mutants, *smt1-1* and *smt1-2*, possessed an *Ac* transposon linked to the mutant phenotype. By DNA gel blot analysis, linkage of the mutant phenotype and *Ac* element was observed in the bulked mutant offspring from an *SMT1*/*smt1-1* heterozygous plant. The genomic sequence flanking the *Ac* insertion in *smt1-1* was isolated by inverse polymerase chain reaction (PCR), as described in Methods. As shown in Figure 5A, in either of the two mutants *smt1-1* or *smt1-2*, a single *Ac* transposon insertion and the resulting DNA restriction fragment length polymorphisms are located in a genomic region, bacterial artificial chromosome (BAC) clone MSH12 (Genbank accession number AB006704), previously sequenced by the international Arabidopsis Genome Initiative (AGI). These two insertions fall within the same predicted gene, MSH12.10, that is highly homologous to a previously characterized soybean C-24 SMT (Shi et al., 1996).

All four mutants have alterations in the *SMT1*/MSH12.10 open reading frame that are likely to result in the complete absence of SMT1 function. The *smt1-1* allele results from an insertion of an *Ac* element in the second intron of *SMT1*. The *Ac* element in *smt1-1* is presumably immobilized by a small deletion of its 5′ end. In addition, the *Ac* element in *smt1-1* is flanked by an unusual 222-bp genomic duplication.

The *smt1-2* allele results from an *Ac* insertion in exon 12. The transposon is flanked by an 8-bp genomic duplication that is typical of the targets of *Ac* insertion. The *smt1-2*/*smt1-2* plants are unstable and give rise to revertant progeny with a wild-type phenotype. The instability of homozygous *smt1-2* strains is best explained by the presence of an active *Ac* transposon in the mutant. Upon further testing, some wild-type revertants among the progeny of *smt1-2*/*smt1-2* plants proved to be heterozygous for *smt1* (*SMT1*/*smt1-2*) but remained homozygous for the linked hygromycin-resistance marker. The faint band in the *smt1-2* DNA lane in Figure 5A, corresponding to the wild-type-size genomic fragment, is molecular evidence for the active *Ac* transposition, which is presumably responsible for reversion events. The overall growth of soil-grown *smt1-2*/*smt1-2* plants tends to be better than that of the other three mutants—probably because of frequent somatic excision of the *Ac* allele to yield wild-type sectors.

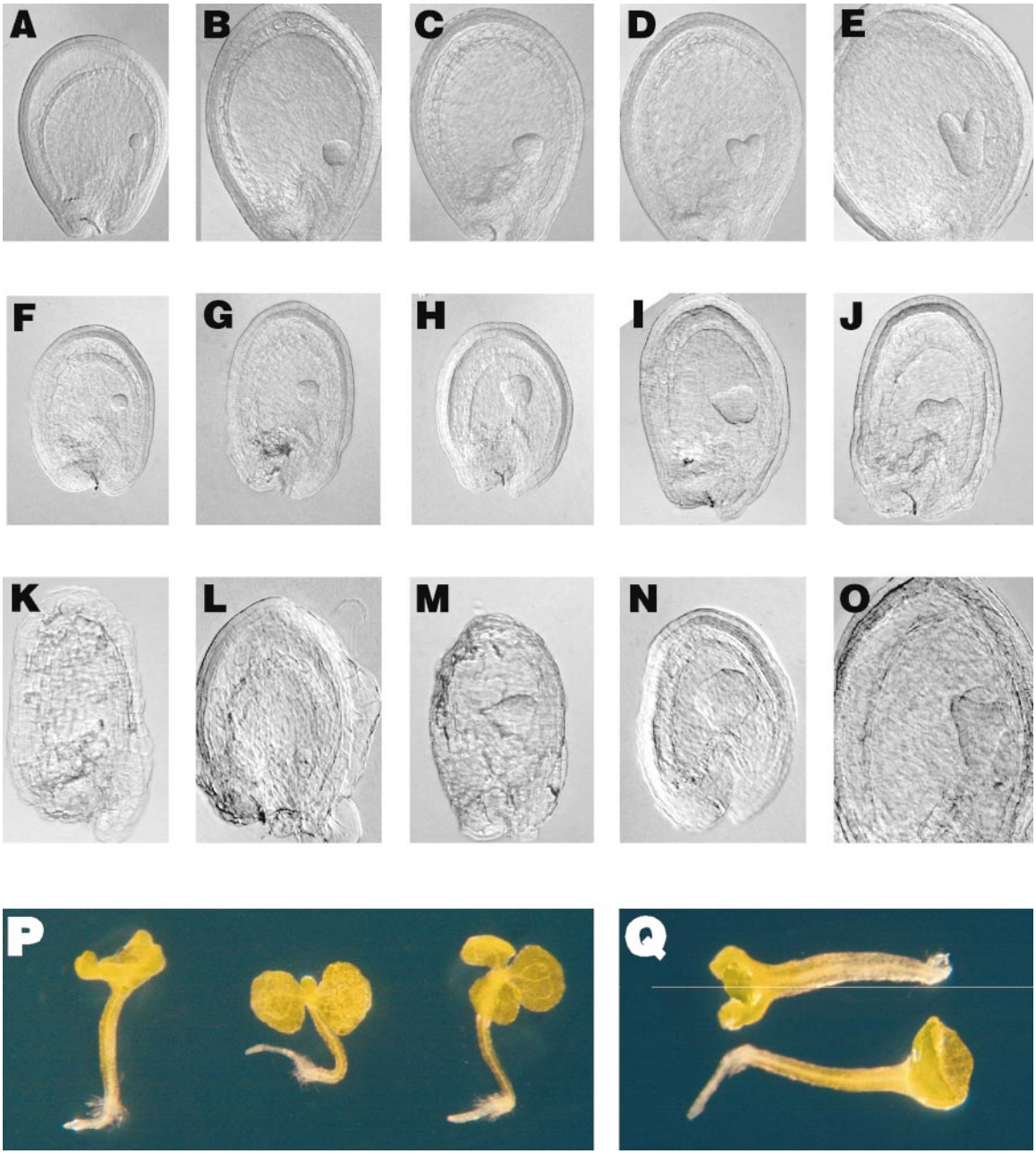

Figure 4. *smt1* Is Defective in Embryogenesis.

(A) to **(J)** The embryos of wild-type *SMT1* (**[A]** to **[E]**) and *smt1* (**[F]** to **[J]**).
(B) and **(F)** Early globular stage.
(C) and **(G)** Midglobular stage.
(D) and **(H)** Late globular stage.
(E) and **(I)** Heart stage.
(F) and **(J)** Late heart stage.
(K) to **(O)** Examples of awry embryogenesis in *smt1* siliques.
(K) and **(L)** Extensive necrosis and cellular swelling of embryo sac with early globular stage embryo.
(M) Extensive necrosis of embryo sac with heart stage embryo.
(N) A massive globular embryo lacking any of the form of wild-type embryos.
(O) Late heart stage embryo with three cotyledons forming at the apex.

The *smt1-3* allele contains no *Ac* insertion; instead, a short sequence duplication and a single base pair insertion in exon 10 shift the reading frame and give rise to a nonsense codon (TGA) close to the site of the mutation. The DNA lesion in *smt1-3* is likely to have arisen from excision of *Ac*. The *smt1-4* allele is a complex DNA rearrangement (deletion and insertion) that is also likely to be the aftermath of an *Ac* excision (Figure 5B). All four alleles lead to a similar phenotype, probably the null phenotype, because each is likely to lead to complete loss of function.

SMT1 Transcript and Protein Sequence

The nucleotide sequence of the open reading frame in the *SMT1* cDNAs was identical to the sequence reported for MSH12.10 by AGI. The exon and intron boundaries of *SMT1*/MSH12.10 were as predicted by AGI except for an additional intron and exon, containing an untranslated sequence, at the 5′ end. *SMT1* encodes the same polypeptide motifs common to *SMT2*, *SMT3*, *ERG6*, and all previously reported SMTs. However, as shown in Figure 6, the polypeptide sequence of *SMT1* resembles the class one SMTs more than do the other two Arabidopsis SMTs, *SMT2* and *SMT3*. As is the case with other SMTs that catalyze the first methyl-transfer reaction preferentially to the second methyltransfer reaction, *SMT1* is more related to the yeast SMT *ERG6* than to the two other Arabidopsis SMTs, which preferentially generate the 24-ethyl sterol side chain.

SMT1 Transgenes Complement *smt1-3*

Transgenic *smt1-3*/*smt1-3* plants containing constructs derived either from a genomic clone of *SMT1* or from an *SMT1* cDNA have a wild-type phenotype. One construct contained a transgene with the *SMT1* locus on the HindIII genomic fragment, depicted in Figure 5B. This genomic segment of *SMT1* completely complemented the *smt1-3* allele in homozygous *smt1-3*/*smt1-3* plants, as explained in Methods. The AGI annotation, in addition to our own sequence analysis, suggests that this genomic sequence lacks any open reading frame other than *smt1* with significant length or homology to Genbank database entries. The other transgene contains an *SMT1* cDNA inserted in front of the 35S cauliflower mosaic virus (CaMV) promoter in a standard expression construct. Homozygous *smt1-3*/*smt1-3* plants containing the *SMT1* cDNA transgene were essentially wild type in appearance and fertility, except for the persistence of a defect in embryogenesis. This defect in embryogenesis could be a consequence of the 35S CaMV promoter, which might lead to abnormal expression of *SMT1* during embryogenesis. Alternatively, intron sequence might be critical for the proper embryonic *SMT1* expression pattern.

SMT1 Encodes SMT Activity

Several in vivo and in vitro assays suggest that the Arabidopsis *SMT1* gene encodes an SMT. *SMT1* suppresses the defects of a yeast mutant (*erg6*) that lacks SMT activity, suggesting that the Arabidopsis gene performs a step in sterol biosynthesis analogous to that performed by Erg6p. Yeast *erg6* strains have several phenotypes such as sensitivity to lithium salt and cycloheximide and resistance to nystatin. In Figure 7, expression of the Arabidopsis *SMT1* cDNA from the *ADH1* promoter in a yeast *erg6* strain partially relieves the sensitivities to lithium acetate and cycloheximide and diminishes the resistance to nystatin. Extracts of *erg6*::*HIS3* yeast strains that express *SMT1* have three prominent 24-methyl sterols, one of which is ergosterol (see Methods).

E. coli strains expressing the *SMT1* cDNA produced SMT activity in crude homogenates, whereas strains lacking the plant gene did not. Using cycloartenol as the sterol substrate, we measured apparent K_m and V_{max} values of 42 μM and 5.2 pmol min^{-1} mg^{-1} protein in Figure 8A for the conversion to 24-methylene cycloartenol (Figure 1, step 1). Whereas 24(28)-methylene cycloartenol was not a suitable substrate, the SMT1-containing extracts did convert 24(28)-methylene lophenol to the 24ε-ethylidene sterol (Figure 1, step 7, and Figure 8B). However, because the second transmethylation in the latter reaction was performed with ~10-fold less efficiency than the first transmethylation with cycloartenol, accurate measurement of kinetic parameters of the first transmethylation reaction was precluded.

smt1-1 Plants Accumulate Cholesterol

The role of *SMT1* in Arabidopsis sterol biosynthesis was determined by comparing the sterol composition of 1-month-old *smt1-1* with wild-type *SMT1* plants (Table 2). The *smt1-1* plants had 25% more mass of sterol per gram of plant material than did the wild-type *SMT1* plants. The most noteworthy difference in the relative content of major sterols is that in *smt1-1* plants, cholesterol is the most abundant sterol

Figure 4. (continued).

(P) and **(Q)** *smt1* seedlings germinated on plant nutrient agar (PNA) and left for 1 month.
(P) Monocot, dicot, and tricot (from left to right).
(Q) Crown cotyledon (above) and ringed cotyledon (below).

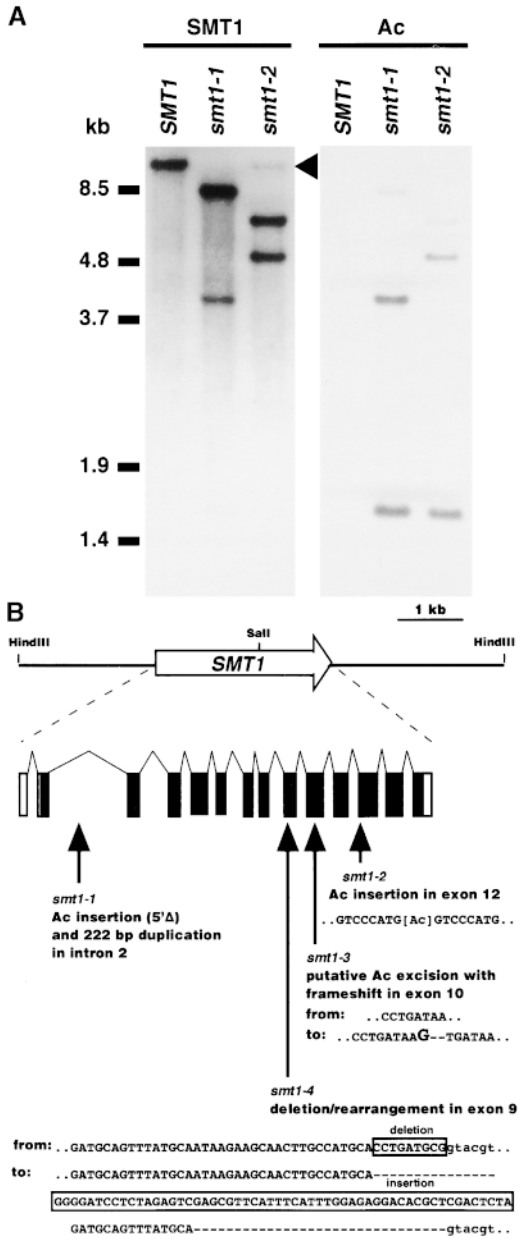

Figure 5. DNA Structure of Four Mutant Alleles of *smt1*.

(A) DNA gel blot hybridization of *smt1-1* and *smt1-2*. Genomic DNA was separated according to size after digestion with HindIII. The nylon blot was hybridized to an *Ac* DNA fragment and then was stripped and hybridized to the *SMT1* cDNA. The gel mobility of molecular weight markers is indicated at left in kilobase pairs (kb).

(B) The location and description of the lesions in the mutants. The HindIII genomic fragment that complements the *smt1-3* is at the top. The lefthand HindIII-SalI fragment was fused to *uidA* in the *SMT1*::*GUS* fusion. (AGI predicts that the very 3′ end of the open reading frame of the next gene MSH12.11 is at the lefthand HindIII site.) The *SMT1* exons are depicted as boxes joined by lines and introns as spacing relative to their nucleotide length. The predicted open reading frame in exon boxes is blackened.

and accumulates at the expense of sitosterol (24-ethyl cholesterol), which ordinarily is the most abundant sterol in Arabidopsis. Surprisingly, though, the campesterol (24-methyl cholesterol) content is relatively unaffected in *smt1-1*. Other than the greater than fourfold increase in cholesterol and reduction in sitosterol, the relative amounts of the other sterols are similar in *smt1-1* and *SMT1* plants. Moreover, the overall content of the dominant C5 sterols (where C5 refers to the desaturation at carbon 5 in the sterol nucleus, a double bond between carbons 5 and 6)—cholesterol, campesterol, sitosterol, and 24-methylene-cholesterol, which all have the same polycyclic ring structure—is the same 80% in both *smt1-1* and *SMT1* wild type. Nevertheless, some minor sterol intermediates, including cholesta-7-enol and 14-methyl-cholesta-8-enol, do show low but unusual accumulation (Table 2).

smt1 Seedlings Are Sensitive to Brassinosteroid

The *smt1* plants have short hypocotyls, a phenotype typical of brassinosteroid-deficient mutants such as *det2* and *dwf1* (Fujioka et al., 1997; Klahre et al., 1998; Choe et al., 1999a). Given *smt1-1*'s defect in sterol biosynthesis, we compared *smt1* with *det2* and *dwf1* to determine whether these mutants had similar responses to exogenous brassinosteroid on the hypocotyl and primary root. In Figure 9, epibrassinolide (100 nM) stimulated hypocotyl length of the *det2* or *dwf1* dwarf mutant to increase 5.5- or 4.5-fold, respectively, whereas the hypocotyl length of *smt1-3* showed only a modest 1.8-fold increase. However, the epibrassinolide stimulation in *smt1-3* was still greater than that seen for hypocotyl elongation in the wild type (a 1.2-fold increase). Similar effects on hypocotyl growth were observed for etiolated seedlings of the mutants and wild type on medium containing epibrassinolide (up to 500 nM).

Epibrassinolide is extremely inhibitory to the *smt1* roots as compared with the wild type (Figure 9). *smt1-3* root growth was greatly inhibited at epibrassinolide concentrations (10 nM) that fail to inhibit the wild type. These results suggest that roots of *smt1* are hypersensitive to epibrassinolide.

One explanation for the phenotype of *smt1* roots is that they accumulate toxic amounts of brassinolides. However, attempts to reduce the endogenous brassinolide biosynthesis of *smt1*, by introducing the *det2* mutation into the *smt1* background, failed to improve the poor growth of *smt1-3* roots. The *smt1-3 det2* double mutant displayed the phenotypic attributes of both mutations: the same abnormal root cell shape and disordered cell files as *smt1,* and the more stunted root elongation of *det2*.

SMT1::*GUS* Expression

To visualize the spatial and relative activity of *SMT1* transcriptional expression, we transformed plants with a con-

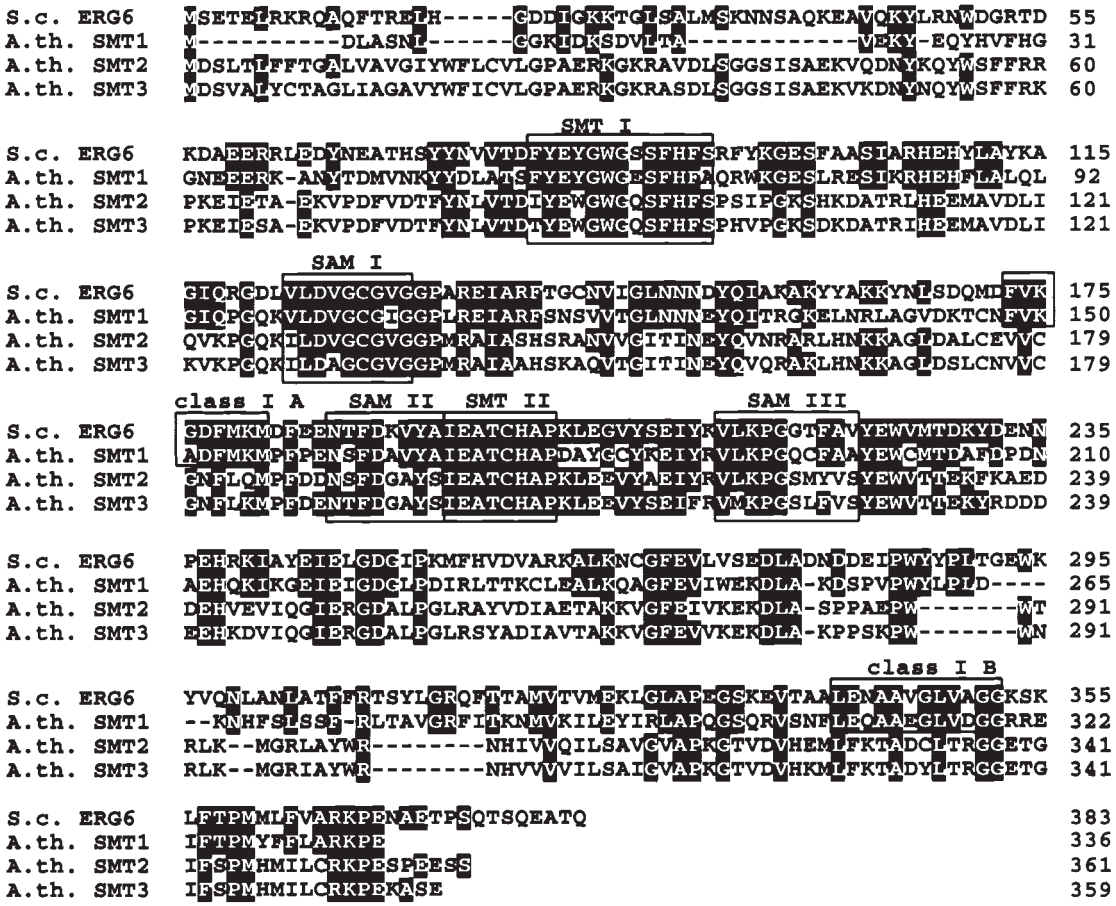

Figure 6. Alignment of SMT Protein Sequences.

The polypeptide sequence of the three Arabidopsis SMTs and the Saccharomyces *ERG6*-encoded protein were aligned using MegAlign software (clustal method; DNAStar). Any residue in *ERG6* identical to an aligned residue in any other SMT is highlighted by white print on black. Seven motifs are boxed and labeled. *S*-Adenosylmethionine–dependent methyltransferases share three motifs: SAM I, SAM II, and SAM III. Two motifs, SMT I and SMT II (invariant), are found in C-24 SMTs. The class one C-24 SMTs in plants are distinguished from class two by two motifs, labeled class I A and class I B (Grebenok et al., 1997).

struct containing a translational fusion of the 5′ intergenic region and the first 73 amino acids of *SMT1* fused to a bacterial *uidA* reporter gene β-glucuronidase (*SMT1*::*GUS*, described in Methods). The staining pattern shown in Figure 10 was essentially the same in two *SMT1*::*GUS* transgenic plant lines from independent transformations, suggesting that the pattern of transcriptional regulation of the gene fusion is contained within the *SMT1*::*GUS* transgene.

The *SMT1*::*GUS* transgene is highly expressed in the vasculature, mature leaves, and regions undergoing cellular expansion, as seen in Figure 10. The vasculature of mature leaves and young roots is darkly stained. In contrast, staining in newly forming leaves and older roots is much diminished or absent. The *SMT1*::*GUS* is expressed only at the apical edge of young leaves; examination of progressively older leaves in the rosette shows the expression spreading toward the petioles, suggesting that expression spreads in the direction of progressive maturation and expansion of leaf cells, beginning at the apex.

Detectable *SMT1*::*GUS* expression was absent from most of the inflorescence, elongating petals, filaments, and the outer carpel walls. No expression was observed inside carpels, either in the ovary sac or embryo sac before or after pollination.

Expression of *SMT1* and *SMT3* Transcripts

The *SMT1* RNAs as detected by RNA gel blot analysis (Figure 11) were detected throughout the plant, including roots (A.C. Diener, unpublished results) and different shoot parts. The RNA expression of *SMT1* is strongest in growing regions of the plant, especially the shoot apex, where

SMT1::*GUS* expression is conspicuously absent. The transcripts of the two other SMT genes in Arabidopsis, *SMT2* (A.C. Diener, unpublished results) and *SMT3*, are also broadly expressed throughout the plant. No *SMT1* transcript appears to accumulate in *smt1-1* plants in which an *Ac* insertion sits near the 5′ end of *SMT1*; a small amount of *SMT1* transcript appears in *smt1-3*, in which a frameshift truncates the SMT1 after amino acid 209 by adding a single lysine residue to the C terminus. The greater amount of *SMT3* RNA in *smt1-1* plants than in *smt1-3* plants, as seen in Figure 11, was observed in several different experiments. Although *smt1-1* and *smt1-3* are morphologically identical, RNA accumulation of *SMT3* (and *SMT2*; A.C. Diener, unpublished results) is greater than in the wild type in plants with the *smt1-1* allele but not in plants with the *smt1-3* allele. The amount of expression of all three *SMT* genes in Arabidopsis is also unaffected in 3.5-week-old *dwf1* plants, a dwarf mutant deficient in a enzymatic activity immediately downstream of the *SMT*s (A.C. Diener, unpublished results).

SMT Expression in Embryos

All three SMT genes have strong and spatially distinct expression in developing embryos, as detected by the in situ RNA hybridization shown in Figure 12. We could detect RNA for the *SMT* genes in both early (heart stage; W.J. Whorisky, unpublished results) and later stage embryos, in which expression domains for each were more clearly demarcated. *SMT1* RNA is strongly expressed below the cotyledons and much less so in the cotyledons (Figures 12A to 12D). *SMT2* RNA is strongly expressed throughout the developing embryo (Figures 12E to 12H). *SMT3* RNA is expressed strongly in the hypocotyl and radicle primordium but is excluded from the central vasculature; in the cotyledons, *SMT3* RNA expression is strongest at the apical tips (Figures 12I to 12L). Because of the strong embryonic phenotypes, we suspect that these RNA patterns reflect SMT1 protein expression in the embryos, despite the lack of detection in the carpels or embryo sac with the *SMT1*::*GUS* fusion.

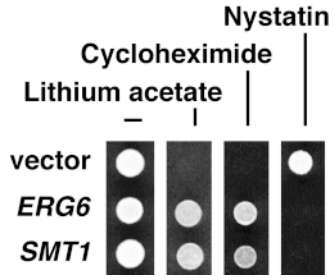

Figure 7. Arabidopsis *SMT1* Suppresses Phenotypes of a Saccharomyces *erg6*::*HIS3*.

Equivalent dilutions of overnight cultures were spotted on basal medium or basal medium containing lithium acetate (50 mM), cycloheximide (50 μg/L), or nystatin (20 mg/L). The *erg6*::*HIS3* strain harbored either a 2 μm vector control plasmid or a 2 μm plasmid expressing the Arabidopsis *SMT1* cDNA or the yeast *ERG6* coding region. After 2 days at 30°C, growth on the plates was photographed.

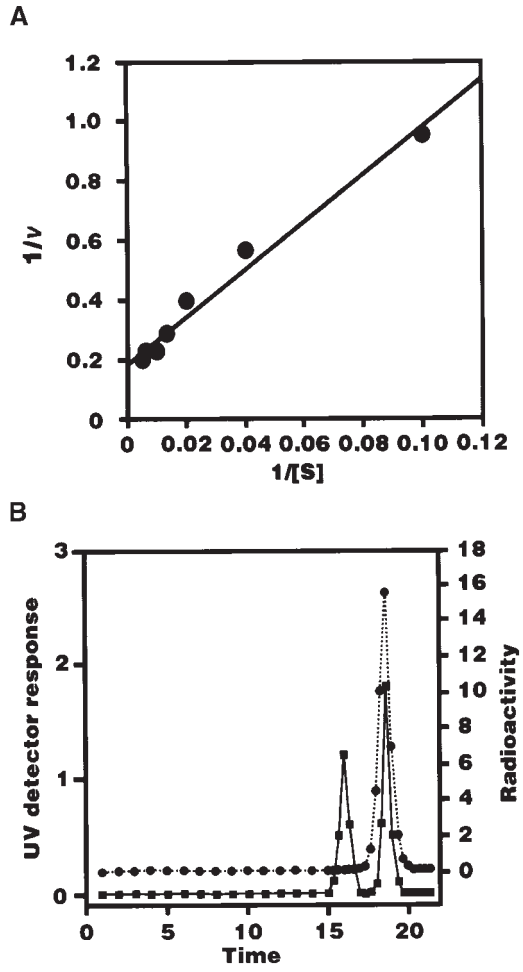

Figure 8. SMT1 Enzymatic Activity.

(A) Lineweaver-Burk plot of the kinetics of SMT1 activity. The concentration (μM) of the substrate cycloartenol (S) was varied, whereas the concentration of [methyl-^{3}H]*S*-adenosylmethionine (SAM) was fixed (50 μM). The vertical axis is the inverse of the rate of radioactive incorporation (θ, pmol min^{-1} mg^{-1} protein).

(B) HPLC radioactivity count (×1000 dpm, circles and dotted line) versus mass representation (squares and solid line) of the product of sterol C-24 methylation after incubation of SMT1 with 50 μM each of [methyl-^{3}H]SAM and 24(28)-methylene lophenol. The fractions corresponding to sterol containing radioactivity were pooled and injected into a second reversed phase. The first mass peak corresponds to the elution time of authentic 24(28)-methylene lophenol, and the second mass peak corresponds to the elution time of authentic citrastadienol (24-ethylidene lophenol).

DISCUSSION

There are three genes for C-24 SMT (*SMT1*, *SMT2,* and *SMT3*) in Arabidopsis. No other family members could be detected by PCR amplification with a set of degenerate primers to highly conserved motifs in *SMT* genes, by low stringency hybridization to genomic DNA gel blots with *SMT1*, *SMT2,* or *SMT3* probes, or by sequence database searches (A.C. Diener, unpublished results). The SMT activity of *SMT2* and *SMT3* was previously analyzed by heterologous expression in yeast and in extracts of *E. coli* expressing a cDNA of *SMT2* (Husselstein et al., 1996; Bouvier-Nave et al., 1997; Tong et al., 1997). The closely related SMT2 and SMT3 proteins have been proposed to perform in planta specifically the second C-methyl addition (Figure 1, step 7), based on the substrate preference of their enzymatic activity (Bouvier-Nave et al., 1998). Our analysis of the *SMT1* gene suggests that SMT1 preferentially catalyzes the first methyl addition (Figure 1, step 1).

Evidence for the functional assignment of SMT1 comes from several experiments. For example, *SMT1* suppresses many of the phenotypes associated with the yeast *erg6* mutation. Moreover, expression of *SMT1* in *erg6* cells leads to the synthesis of 24-methyl sterols that are not present in the *erg6* mutant when the Arabidopsis *SMT1* gene is not included. In contrast, the predominant sterols when Arabidopsis *SMT2* was expressed in *erg6* were C-24 ethylated species. A first methyl addition by SMT1 is further supported by the observation that *SMT1* activity expressed in *E. coli* acted to catalyze a SAM-dependent transmethylation of cycloartenol. The SMT1 protein obtained from *E. coli* showed ~10-fold less methyltransferase activity with 24-methylene lophenol than with cycloartenol. These data, supporting a preference for the first methyl addition activity, agree with earlier data obtained with the tobacco class one SMT Ntsmt1-1 (Bouvier-Nave et al., 1998).

The pattern of accumulation of sterols in *smt1* is also consistent with a defect in C-24 transmethylation. In *smt1-1* plants, cholesterol accounts for one-fourth of all sterol and accumulates at the expense of sitosterol; the amount of campesterol, however, is unaffected. Given that *smt1* has lost methyltransferase activity, the accumulation of cholesterol, which lacks C-24 alkylation, is reasonable. However, the deficiency in sitosterol (a C-24 ethylated sterol) and the nearly normal accumulation of campesterol (a C-24 methylated sterol) are unexpected. Actually, if SMT1 were the only enzyme responsible in planta for the first transmethylation reaction of cycloartenol to produce 24-methylene cycloartenol, *smt1-1* should be completely deficient for C-24 alkylation because the second transmethylation reaction occurs only after the first transmethylation reaction. Because the majority of sterols in *smt1-1* plants are alkylated, *SMT1* cannot be the only enzyme in Arabidopsis capable of the first C-24 methylation step.

One explanation for the accumulation of methylated sterols in *smt1* is that in the absence of SMT1, these methylations are performed by other enzymes that do not ordinarily perform this reaction in the wild type. The ability of enzymes to act as "imposters" has been described in the mitogen-activated protein kinase pathway of yeast and may be a more general phenomenon (Madhani et al., 1997). In the wild type, the protein interactions of the SMT1 enzyme may exclude the other potential SMTs, namely, SMT2 and SMT3, from target substrates. In *smt1*, however, the other enzymes, although with perhaps lower affinity, may now have access to these substrates and perform methylations—albeit at a different rate and with different affinities.

These considerations bear directly on the relationship between the two sequence-related classes of plant *SMT* genes and the two SMT activities. The question is whether the division by sequence relatedness reflects a rigid functional difference. The ascomycete fungus *S. cerevisiae* produces only C-24 methylated sterols by the SMT Erg6p, a yeast protein for which the amino acid sequence is more closely related to that of the class one plant family of SMT genes than to the class two genes. On the basis of this relatedness, it has been argued that in planta, only the class one plant *SMT* genes perform the first methyl addition. However, the presumption that the more recent divergence of the Arabidopsis SMT1 and Saccharomyces Erg6p protein is related to the restriction of SMT activity to the first transmethylation step deserves some scrutiny. For instance, the Basidiomycete rust *Uromyces phaseoli* is capable of producing sterols with either a C_1 or C_2 addition (Bansal and Knoche, 1981). The inability to separate the first and second

Table 2. Major Sterol Content of Whole Plant

	Fraction of Total Sterol[a]	
Major Sterol	*SMT1*[b]	*smt1-1*[c]
Sitosterol	48	22
Campesterol	20	21
Isofucosterol	10	15
Cycloartenol	10	9
Cholesterol	6	26
24-Methylene-cholesterol	5	10
Fucosterol	1	1
24-Methylene-cycloartenol	Trace	Trace
Cholesta-7-enol	ND[d]	3
Cholestanol	ND	1
14-Methyl-cholesta-8-enol	ND	1
Sitostanol	Trace	Trace
Campestanol	Trace	Trace

[a] Expressed as a percentage.
[b] Wild-type *SMT1* plants contained 179 μg/g fresh weight.
[c] Mutant *smt1-1* plants contained 223 μg/g fresh weight. The *smt1-1* plants are morphologically different from the wild type, and these tissue differences may influence the total sterol content.
[d] ND, not determined.

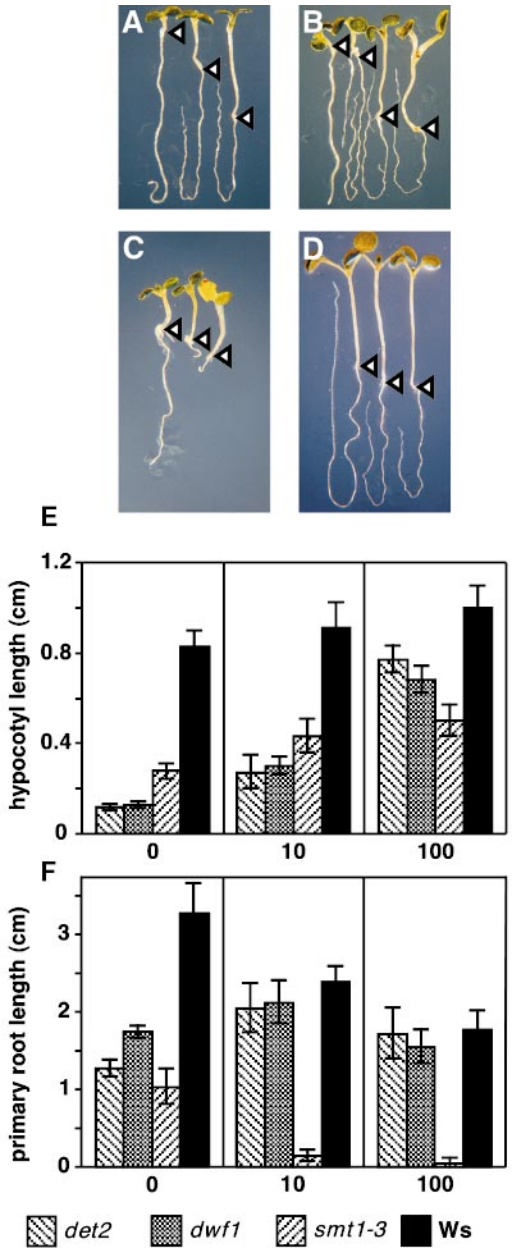

Figure 9. Sensitivity to Brassinosteroid.

(A) to **(D)** Different ecotypes of plants grown for 1 week at 22°C under yellow light on PNG medium supplemented with (from left to right) 0, 10, or 100 nM epibrassinolide. Triangle points mark the hypocotyl–root junction.
(A) det2.
(B) *dwf1.* Shown are two seedlings on 100 nM epibrassinolide.
(C) smt1-3.
(D) Ws ecotype.
(E) and **(F)** Hypocotyl and root lengths, respectively, for each mutant; values are an average of at least 8 seedlings. Error bars represent the standard deviation.

transmethylation reactions of *U. phaseoli* by chromatographic schemes led to the conclusion that both activities reside in the same protein complex; furthermore, both of the Uromyces SMT activities shared identical sensitivities to various salts and detergents. It is conceivable, therefore, that the progenitor of Saccharomyces *ERG6* and the Arabidopsis *SMT1* gene might have been responsible for both C_1 and C_2 alkyl additions. By this argument, the Saccharomyces *ERG6* has since lost the ability to perform both steps and has evolved into an enzyme capable of only the first methyltransferase reaction. In support of this contention, a single conserved amino acid change in *ERG6* has been found to impart a C_2 addition activity (Nes et al., 1999).

The phenotype of *smt1* adds to the increasing knowledge about the biological importance of sterols in plants. *smt1*, like the other two Arabidopsis mutants specifically defective in sterol biosynthesis (*dwf1*/*dim*/*cbb1* and *ste1*/*dwf7*) (Gachotte et al., 1995; Kauschmann et al., 1996; Klahre et al., 1998; Choe et al., 1999a, 1999b), results in small plants. However, *smt1* does not share the distinctive dwarf appearance of the brassinolide-deficient *dwf1* and *dwf7*. Moreover, the morphological phenotypes of *dwf1* and *dwf7* are rescued by brassinosteroid, whereas the *smt1* defect is not (Choe et al., 1999a, 1999b).

The reduced hypocotyl length of *smt1* is only modestly affected by exogenous epibrassinolide, as compared with the more dramatic effect of epibrassinolide on mutants *det2* and *dwf1*. Actually, both *smt1* and wild-type plants accumulate about the same amount of campesterol, the immediate sterol precursor of brassinolide. Of course, these observations discount only the possibility of an exclusive defect in brassinolide biosynthesis. Already in the developing embryo, strikingly distinct patterns of expression were seen for the three *SMT* RNAs, and again, in the rosette, we observed stronger *SMT1* expression in leaves undergoing expansion. The mild restriction of growth of the leaves or stems may reveal a subtle and local deficiency for brassinosteroid.

Restricted accumulation of alkylated dominant sterols is the most dramatic effect of the *smt1* mutation. The first SMT C_1 reaction is the first biosynthetic step in sterol transformation (Figure 1), yet in *smt1*, most sterol accumulates as cholesterol, a natural but minor dominant sterol, and not as cycloartenol, the immediate precursor of the first SMT reaction. Compromised transmethylation in *smt1* plants failed to restrict further sterol transformation (Benveniste, 1986; Bach and Benveniste, 1997). Irregular regulation of sterol synthesis by the skewed pattern of C-24 alkylation may explain the apparent 25% overabundance of sterols in *smt1-1* plants. However, with the caveat that we have not ascertained the subcellular distribution of sterols in *smt1* plants, the enumerated *smt1* defects may be attributed specifically to a reduction in C-24 alkylation and not to the absence of the normally dominant C5-sterols, because 80% of sterols in both *smt1* and wild-type plants have the normal C5 polycyclic ring structure.

Among sterol modifications, C-24 alkylation appears to be

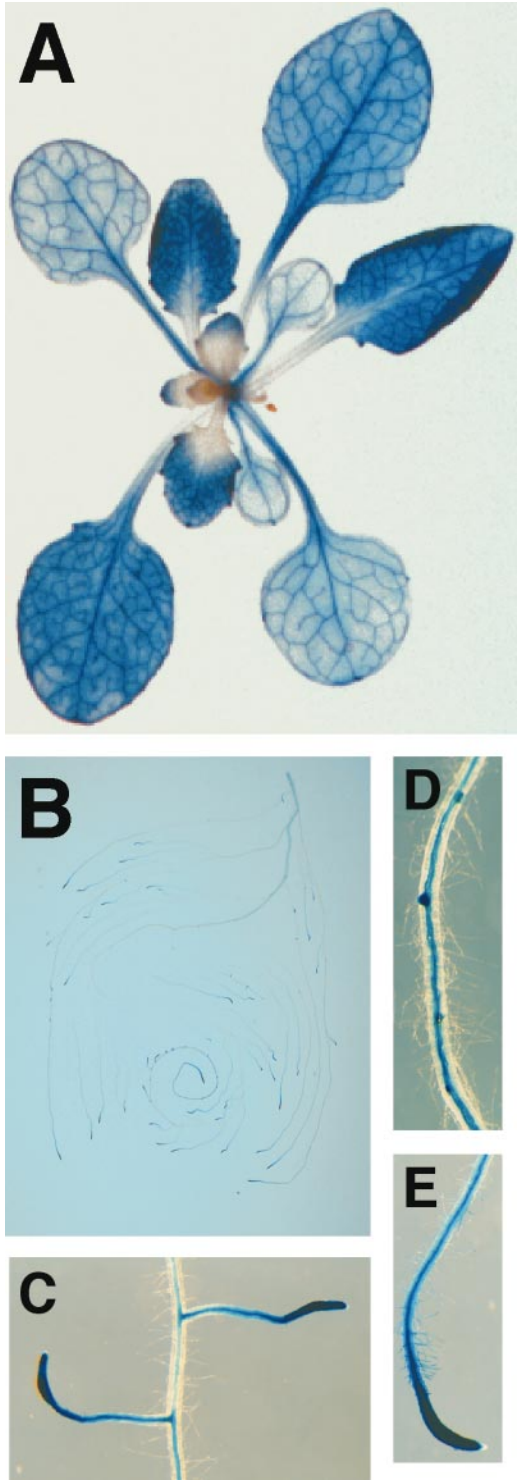

Figure 10. Expression of *SMT1*::*GUS* in Transgenic Plants.

Three-week-old *SMT1*::*GUS* plant indigo-stained with X-Gluc and cleared of endogenous pigments.
(A) The aerial half of the plant.
(B) The whole root system.
(C) Newly formed lateral roots.
(D) Lateral root primordia within root.
(E) The root apical end.

especially critical for sterol membrane function; its deficiency in *smt1* is probably responsible for the altered membrane properties and the phenotypes associated with the mutation. We have found that *smt1* roots are hypersensitive to calcium salts and epibrassinolide and that *smt1* root growth is affected by some component or condition initially present in agar plates. Work with yeast ergosterol biosynthetic mutants suggests that the lack of C-24 alkylation in *erg6* strains is more consequential to membrane integrity, as assessed by cation sensitivity and dye permeability, than are alterations in sterol B-ring structure affected by either the *erg2* mutation (deficient in C8–C7 isomerization, equivalent to step 6 in Figure 1) or *erg3* (deficient in C5-desaturase activity, equivalent to *STE1*/*DWF7*, step 9 in Figure 1) (Bard et al., 1978). The Arabidopsis *ste1* mutant, deficient in an activity equivalent to that of yeast *ERG3*, has no visible morphological consequence, despite the fact that only 32% of accumulated sterols are the normally dominant C5-sterols, whereas the majority (68%) of sterols are the C5,7-sterols, which are normally intermediate (Gachotte et al., 1995). In the case of the stronger *dwf7*, allelic to *ste1*, virtually all of the mutant phenotype has been attributed to brassinosteroid deficiency because the dwarfism of the mutant can be rescued by supplementation with exogenous brassinosteroid (Choe et al., 1999b).

Maternal fertility and embryogenesis are particularly sensitive to the loss of *SMT1* function. The *dwf7* mutant also has reduced fertility unrelated to its brassinosteroid deficiency (Choe et al., 1999b); however, the nature of the *dwf7* fertility problem awaits more careful examination. The aberrant morphogenesis of the *smt1* embryo may be analogous to the inhibited growth of *smt1* roots on agar: The appearance of the embryonic projections for cotyledons and the hypocotyl/root axis is muted, whereas in the case of the attenuated *smt1* root, cells are short and rounded, failing to form regular files or their normal elongated, rectangular shape. When grown in soil, *smt1* root cells can have normal shape and the roots look like wild-type roots. We speculate, by extension of what is known about the yeast *erg6* mutant, that the altered membrane integrity of *smt1* is responsible for its conditional root phenotype, calcium salt sensitivity of roots, and defects in embryo morphogenesis.

Two problems complicate the analysis of the steroid pathway by molecular genetic approaches. First, the sterol transformation pathway is not a simple linear pathway. For example, a defect in SMT1 alkylation fails to interrupt the further transformation of cycloartenol into the ordinarily dominant C5-sterols. Thus, it is difficult to determine the

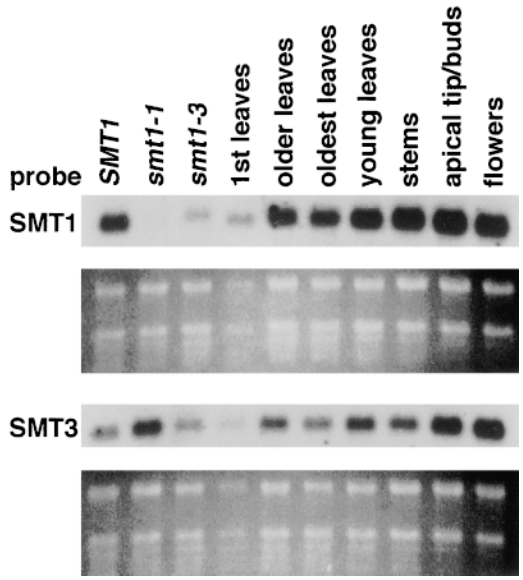

Figure 11. RNA Expression of *SMT1* and *SMT3*.

RNA was size-separated and blotted onto nitrocellulose for RNA gel blot analysis. Ethidium bromide staining of rRNA in each gel accompanies the hybridization. In the first three lanes, rosette leaves were collected for RNA extraction from *SMT1*/*SMT1*, *smt1-1*/*smt1-1*, and *smt1-3*/*smt1-3* plants. In the remaining lanes, RNA was extracted from the aerial part indicated of 2-week-old soil-grown plants.

normal substrates for each enzyme by using as an indication of the precursors those sterols that accumulate in a sterol biosynthetic mutant. Second, in mutants, many of the sterol biosynthetic enzymes may plausibly perform reactions that they do not perform in the wild type. For example, SMT2 and SMT3 may substitute, however poorly, for SMT1 activity in *smt1*. These secondary overlapping activities would be revealed if it were possible to construct strains with mutations in all three *SMT* genes.

The availability of both mutations and genes in the Arabidopsis sterol biosynthetic pathway raises the possibility of manipulating plant sterol biosynthesis. Alterations in sterol composition may lead to improved agricultural varieties and allow the impact of phytosterol intake on animal diet and nutrition to be addressed.

METHODS

Plant Strains and Growth Conditions

The *smt1* mutations, which lack sterol methyltransferase (SMT)–encoding genes, originate from an *Ac* transgenic line in the Wassilewskija (Ws) ecotype. The plants were grown under continuous white light. For germination, and for as long as 3 weeks, plants were usually grown in growth chambers (Controlled Environments, Inc., Pembina, ND) in sterile plates with chemically defined plant nutrient agar (PNA; 5 mM KNO_3, 2.5 mM potassium phosphate, pH 5.5, 2 mM $Ca[NO_3]_2$, 2 mM $MgSO_4$, 50 μM Fe·EDTA, plus micronutrients and 7 g/L Bacto-Agar [Difco]) without or with a 0.5% sugar supplement, either glucose (PNG) or sucrose. After germination, the growth of most *smt1* seedlings was arrested without a carbon energy source. Only about one in 30 *smt1*/*smt1* germinated seedlings turned from pale green to darker green, expanded, and proliferated in the absence of sugar. The arrested seedlings shown in Figures 4P and 4Q were photographed after a month on PNA plates without added sugar. The recipe for 1000 × micronutrient stock is 70 mM H_3BO_3, 14 mM $MnCl_2$, 0.5 mM $CuSO_4$, 1 mM $ZnSO_4$, 0.2 mM Na_2MoO_4, 10 mM NaCl, and 0.01 mM $CoCl_2$. No improvement in *smt1* growth, as compared with the wild type, was observed on medium in which the osmolarity was increased with sucrose or sorbitol or under higher or lower temperatures, at 15, 20, 23, or 28°C, or on medium at pH 6.5 or 7.5. The initial pH of PNA media was controlled by the pH of the potassium phosphate added. The decrease in hypocotyl length of brassinolide-deficient mutants is accentuated by growth under yellow light, which is deficient for blue light. One- or 2-week-old plantlets were transplanted to soil for more extensive growth and seed harvest in a greenhouse with lamp-supplemented continuous lighting. For the germination assays, seeds were stratified for 1 day at 4°C and then grown for 5 days at 22°C under continuous illumination. The *det2* mutant was obtained from the Arabidopsis Biological Resource Center (Ohio State University, Columbus). We took advantage of the tight linkage of *smt1-3* to a hygromycin transgenic marker (see below) to select for the *smt1-3 det2* double mutant. *smt1-3* pollen was crossed onto emasculated *det2* flowers. The F_1 seedlings, unlike the maternal *det2* parent, were hygromycin resistant, confirming the *smt1-3* paternity. The F_2 plants from the self-fertilized F_1 were selected for hygromycin resistance and the dwarf phenotype indicative of brassinolide deficiency. In all cases, the F_3 seedlings of these selected F_2 plants were all dwarfs, and roughly one-quarter of these exhibited embryogenesis defects and root growth abnormalities. This phenotypic segregation was expected from the offspring of a *det2* homozygote and *SMT1*/*smt1* heterozygote.

Plant Transformation

We selected on Luria-Bertani (LB) plates plus 100 mg/L spectinomycin (Sigma) *Agrobacterium tumefaciens* (GV3101) transformed by electroporation with PZP-based vectors (Hajdukiewicz et al., 1994). An initial 5 mL of 2 × LB liquid culture with spectinomycin selection was diluted into 600 mL of 2 × LB without spectinomycin selection, and the cells were grown to saturation. The Agrobacterium cells were pelleted and resuspended in 0.5 × Murashige and Skoog medium (Gibco BRL/Life Technologies) plus 5% sucrose. Secondary inflorescences of Columbia ecotype plants were dipped in Agrobacterium suspension under vacuum for 5 min. Seeds from the transformed plants were selected with 25 mg/L kanamycin B (Sigma).

Nucleic Acids

Unless otherwise noted, all molecular biology protocols were derived from standard protocols (Ausubel et al., 1997). Plant genomic DNA was prepared using a preliminary protocol for genomic DNA extrac-

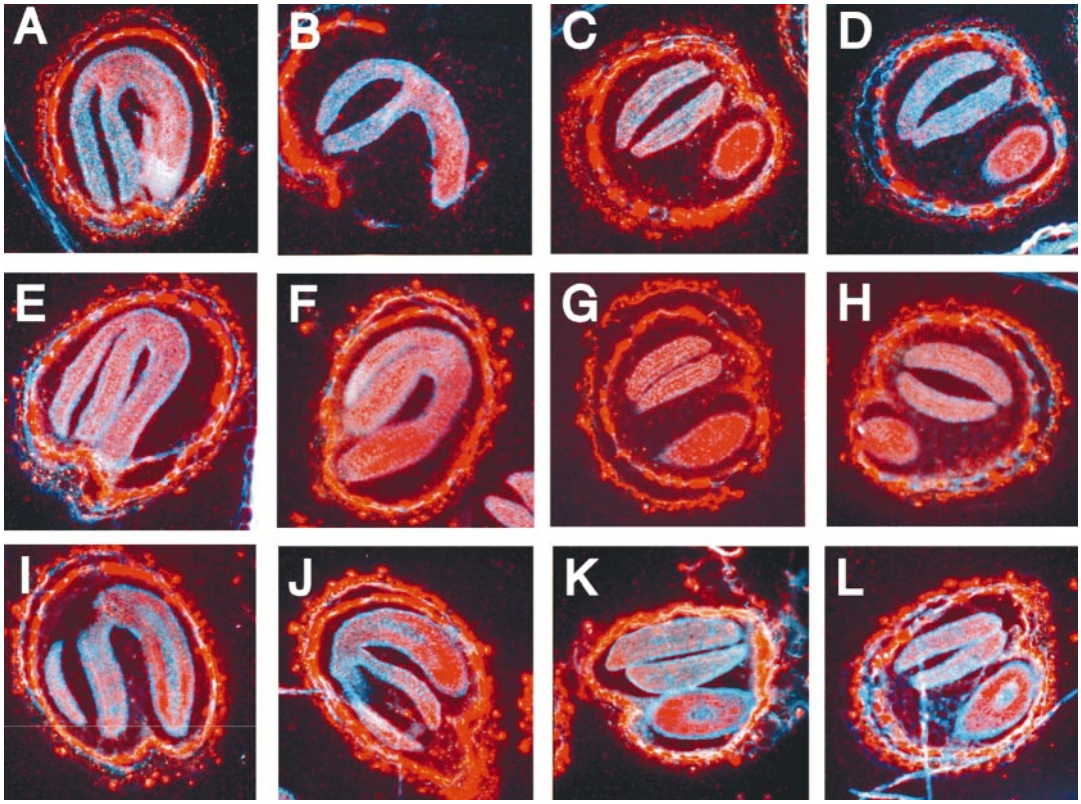

Figure 12. RNA Expression of SMTs in Late-Stage Embryos.

Micrometer sections of siliques with developing embryos were hybridized with antisense RNA probes of cDNA subclones of *SMT1* (**[A]** to **[D]**), *SMT2* (**[E]** to **[H]**), or *SMT3* (**[I]** to **[L]**). The blue color is a fluorescent nuclear stain, and the red color is signal reflected by silver grains.
(A), **(B)**, **(E)**, **(F)**, **(I)**, and **(J)** Approximately longitudinal sections through the embryos.
(C), **(D)**, **(G)**, **(H)**, **(K)**, and **(L)** Cross-sectional cuts through hypocotyl and cotyledons.
The coat of the embryo sac produces a strong background signal. Sense-strand *SMT* probes failed to produce marked signals or signal patterns.

tion from plant leaves with Qiagen-tip (provided by Qiagen, Valencia, CA). Oligonucleotides were purchased from and DNA sequencing was performed by contract with Research Genetics (Huntsville, AL). RNA was extracted from plant material by using Tri Reagent (Molecular Research Center). For DNA gel blot analysis, 2 μg of restriction enzyme–digested DNA was loaded per lane. For RNA gel blot analysis, 5 μg of total RNA was loaded per lane. In situ hybridization was performed as described previously (Geng et al., 1999). The probes for *SMT2* and *SMT3* were derived from the expressed sequence tags 66F6T7 and ATTS3237, respectively, provided by the Arabidopsis Biological Resource Center.

Library Subclones and Plasmid Constructions

Genomic sequence flanking the *Ac* element in *smt1-1* was retrieved by inverse polymerase chain reaction (PCR): 5 μg of *smt1-1* DNA digested with HindIII in 20 μL of reaction medium and ligated in 400 μL. After glycogen coprecipitation, 1/10 of resuspended material served as template for PCR with the primers AD333 (5′-CGGTTATACGATAACGGTCG-3′) and AD334 (5′-GTACGATGAAGTGGTTAGCC-3′). The PCR product of appropriate size was subcloned into Bluescript II vector (BS; Stratagene Inc.) that had been previously digested with EcoRV and treated for subcloning Taq-derived PCR products (Ausubel et al., 1997). This insert served as the probe for hybridization to both a lambda genomic library, in lambda GEM11 (a gift from J.T. Mulligan and R.W. Davis, Stanford University), and a lambda cDNA library, in lambda gt10 (a gift from C. Luschnig, member of Fink laboratory); both libraries were derived from Arabidopsis Columbia ecotype. The 8.4-kb HindIII fragment predicted by the Arabidopsis Genome Initiative (AGI) (depicted in Figure 5B) was subcloned from a lambda genomic clone into BS (BS/SMT/H3) and subsequently into the PZP212 binary vector (PZP/SMT/H3) for plant transformation. Of several cDNA library isolates, cSMT1.13 was completely sequenced and was designated *SMT1* cDNA. The cSMT1.13 sequence consists of nucleotides 7 through 1242 of GenBank accession number AF195648 and was flanked by the linker sequence 5′-GAATTCCCGGGCAGGT-3′ at both ends. For plant expression of *SMT1* cDNA, we digested BS/SMT1.13 with XmaI and ligated the cDNA into the XmaI site of PZP-35S, constructed by inserting the SacI/NsiI fragment containing the 35S promoter and 3′ nos terminator of pART7 into the T-DNA PstI/SacI sites

of PZP212. For the translational fusion of *SMT1* to the *uidA* reporter gene, the 4-kb HindIII/SalI fragment, containing the 5′ intergenic region and first half of *SMT1* from the BS/SMT/H3, was subloned into HindIII- and SalI-digested PZP212/GUS1 vector in which the EcoRI/HindIII T-DNA insert of pBI101.1 was subcloned into EcoRI/HindIII of PZP212. The *Ac* DNA use for a hybridization probe was the PstI insert in pAc3 (a gift from N. Federoff, Pennsylvania State University). For yeast expression, the *SMT1* cDNA was removed from BS/cSMT1.13 with XmaI. We amplified *ERG6* by PCR from yeast genomic DNA by using the primers AD421 (5′-GCGAATTCCCGGGCAGCATAAGATGAGTG-3′) and AD422 (5′-GCGAATTCCCGGGTATATATCGTGCGCTT-3′) and digested the product with XmaI. We then subcloned *ERG6* or *SMT1* cDNA into XmaI between the *ADH1* promoter and terminator in the pAD4M 2-μm plasmid (with *LEU2* marker) for yeast expression (Ballester et al., 1989).

Yeast Strains and Growth Conditions

Unless otherwise stated, yeast strains were grown in standard conditions and analyzed by established techniques (Guthrie and Fink, 1991). We created a 153-bp deletion and *HIS3* disruption of the *ERG6* gene (*erg6*::*HIS3*) by subcloning a *HIS3* gene fragment, removed from pJH-H1 (B1683 in lab collection) with XmaI and ApoI digestion, into pBS/ERG6 plasmid digested with AgeI and MfeI. For *erg6*::*HIS3* disruption, His^+ colonies were selected from the yeast strain 10556-4A *MATa ura3-1 leu2-3,112 his3-11,15* transformed with the disruption construct linearized with XmaI. Leu^+ colonies were selected for transformation of the *erg6*::*HIS3* strain with the pAD4M-based expression constructs.

To assay the suppression of *erg6* sensitivities and resistance, 5-μL drops of a fivefold dilution series (in water) from a saturated liquid yeast culture grown overnight in synthetic complete media minus histidine and leucine with dextrose (SD-HIS-LEU) were added in parallel to SD-His-Leu agar plates alone or with added lithium acetate (50 mM), cycloheximide (50 μg/L), or nystatin (20 mg/L). After ~2 days at 30°C, the yeast growth on the plates was photographed. The suppression of *erg6* by *SMT1* was only partial; in our assays, the yeast *ERG6* in an equivalent context (expressed on plasmid with the *ADH1* promoter) showed stronger suppression. Another class one SMT from *Zea mays* also partially suppressed an *erg6* strain (Grebenok et al., 1997).

smt1-3 Complementation with Transgenes

The *smt1* mutation is tightly linked to the hygromycin resistance marker from the transgene that introduced the *Ac* element, which we confirmed in the *smt1-3* backcross F_2 population. Both transgenes made for complementation-conferred kanamycin resistance to Columbia ecotype after transformation. Therefore, in crosses, we monitored the expression of *smt1-3* and transgenes by assessing resistance to hygromycin (16 mg/L) and kanamycin (25 mg/L), respectively. In lines homozygous for hygromycin (*smt1-3*) resistance and hemizygous for kanamycin resistance, the Smt phenotype segregated with Smt^+ segregating with kanamycin resistance.

Staining of *SMT1*::β-Glucuronidase Transgenic Plants

After 3 weeks of growth on PNA plates, *SMT1*::β-glucuronidase (*GUS*) transgenic plants were submerged in GUS staining buffer plus 0.2 mg/L X-Gluc (Rose Scientific Ltd.); the tissues were infiltrated with staining buffer under vacuum and incubated overnight at 36°C (Jefferson et al., 1987). After rinses with water, we cleared the tissue with ethanol:acetic acid (9:1 [v/v]) and followed this with washes with 90, 70, and 50% diluted ethanol. The tissues were then left in 50% glycerol for later photography.

Light Microscopy

Whole plants were observed and photographed under an M5A Wild Heerbrugg (Leica, Englewood, CA) microscope equipped for photography. Siliques were fixed overnight in an ethanol:acetic acid (9:1) solution, rinsed in 90 and 70% ethanol, and cleared with chloral hydrate:glycerol:water (8:1:2 [v/v]) solution. The cleared siliques were opened on a microscope slide, and the seeds were teased out of the silique. Embryos were visualized by using a Zeiss Axiophot (Carl Zeiss, Thornwood, NY) microscope equipped for photography.

Sterol Enzymology and Analysis

Expression of the *SMT1* cSMT1.13 cDNA in *Escherichia coli* and subsequent biochemical analysis of protein extracts were performed as previously described (Nes et al., 1991, 1998a; Tong et al., 1997). The conditions of the experiments were as follows. A fixed concentration of [*methyl*-^{3}H]SAM (50 μM) was added, along with various concentrations of cycloartenol (10, 25, 50, 75, 100, 150, and 200 μM) in Tween 80 (0.1% v/v), to a homogenate preparation of enzyme derived from *E. coli,* pH 7.5. Each incubation was performed at 30°C for 45 min. The protein concentration in each homogenate suspension was ~1.5 mg/mL. The SMT-generated product, 24ε-ethylidene lophenol, was established by HPLC radiocounting (C_{18}-Whatman column eluted with methanol at ambient temperature), which indicated a single peak of radioactivity coinciding with a mass peak corresponding to a known specimen of 24ε-ethylidene lophenol. The combined nonsaponifiable lipid fraction from a preparative-scale incubation (300 assays) was diluted with 50 μg of 24-ethylidene lophenol to serve as carrier, and the sample was injected into a C_{18}-Zorbax (Hewlett Packard, Palo Alto, CA) semipreparative column eluted with methanol. The HPLC conditions are not sufficiently sensitive to distinguish the geometry of the 24(28)-ethylidine bond. The sterols in the *SMT1*-expressing *erg6* strain described above were analyzed as previously described (Nes et al., 1999). Three gas–liquid chromatographic peaks corresponded to 24-methylated sterols; based on their mass spectra, these were ergosterol, 24(28)-methylene-24,25-dihydrolanosterol, and 4,4-dimethylcholesta-8,14,24(28)-trienol. The structure of the sterols from Arabidopsis plants was established by comparison with authentic specimens (Guo et al., 1995).

ACKNOWLEDGMENTS

A.C.D. is grateful for the in situ RNA hybridization analysis performed in the laboratory of Peter Sicinski at the Dana Farber Cancer Institute (Boston, MA). Many members of the Fink laboratory collaborated to generate the transposon-mutagenized seed from which the *smt1* mutants were isolated. A.C.D. thanks fellow members of the Fink laboratory, especially Amir Sherman for consultation and Kendal Hirschi and Jian Hua for critical reading of the manuscript. This research was supported by National Science Foundation Grant No. MCB-7876367

to G.R.F. The support of W.D.N. by the Welch Foundation (Grant No. D1276) is gratefully acknowledged.

Received December 22, 1999; accepted April 4, 2000.

REFERENCES

Ausubel, F.M., Brent, R., Kingston, R.E., Moore, D.D., Seidman, J.G., Smith, J.A., and Struhl, K. (1997). Current Protocols in Molecular Biology, Vols. 1–3. (New York: John Wiley).

Bach, T.J., and Benveniste, P. (1997). Cloning of cDNAs or genes encoding enzymes of sterol biosynthesis from plants and other eukaryotes: Heterologous expression and complementation analysis of mutations for functional characterization. Prog. Lipid Res. **36,** 197–226.

Ballester, R., Michaeli, T., Ferguson, K., Xu, H.P., McCormick, F., and Wigler, M. (1989). Genetic analysis of mammalian GAP expressed in yeast. Cell **59,** 681–686.

Bansal, S.K., and Knoche, H.W. (1981). Sterol methyltransferase from *Uromyces phaseoli*: An investigation of the first and second transmethylation reactions. Phytochemistry **20,** 1269–1277.

Bard, M. (1972). Biochemical and genetic aspects of nystatin resistance in *Saccharomyces cerevisiae*. J. Bacteriol. **11,** 649–657.

Bard, M., Lees, N.D., Burrows, L.S., and Kleinhans, F.W. (1978). Differences in crystal violet uptake and cation-induced death among yeast sterol mutants. J. Bacteriol. **135,** 1146–1148.

Benveniste, P. (1986). Sterol biosynthesis. Annu. Rev. Plant Physiol. **37,** 275–308.

Bloch, K.E. (1983). Sterol structure and membrane function. CRC Crit. Rev. Biochem. **14,** 47–82.

Bouvier-Nave, P., Husselstein, T., Desprez, T., and Benveniste, P. (1997). Identification of cDNAs encoding sterol methyl-transferases involved in the second methylation step of plant sterol biosynthesis. Eur. J. Biochem. **246,** 518–529.

Bouvier-Nave, P., Husselstein, T., and Benveniste, P. (1998). Two families of sterol methyltransferases are involved in the first and the second methylation steps of plant sterol biosynthesis. Eur. J. Biochem. **256,** 88–96.

Castle, M., Blondin, G., and Nes, W.R. (1963). Evidence for the origin of the ethyl group of β-sitosterol. J. Am. Chem. Soc. **85,** 3306–3308.

Choe, S., Dilkes, B.P., Gregory, B.D., Ross, A.S., Yuan, H., Noguchi, T., Fujioka, S., Takatsuto, S., Tanaka, A., Yoshida, S., Tax, F.E., and Feldmann, K.A. (1999a). The Arabidopsis *dwarf1* mutant is defective in the conversion of 24-methylenecholesterol to campesterol in brassinosteroid biosynthesis. Plant Physiol. **119,** 897–907.

Choe, S., Noguchi, T., Fujioka, S., Takatsuto, S., Tissier, C.P., Gregory, B.D., Ross, A.S., Tanaka, A., Yoshida, S., Tax, F.E., and Feldmann, K.A. (1999b). The Arabidopsis *dwf7/ste1* mutant is defective in the delta7 sterol C-5 desaturation step leading to brassinosteroid biosynthesis. Plant Cell **11,** 207–221.

Fujioka, S., Li, J., Choi, Y.H., Seto, H., Takatsuto, S., Noguchi, T., Watanabe, T., Kuriyama, H., Yokota, T., Chory, J., and Sakurai, A. (1997). The Arabidopsis *deetiolated2* mutant is blocked early in brassinosteroid biosynthesis. Plant Cell **9,** 1951–1962.

Gaber, R.F., Copple, D.M., Kennedy, B.K., Vidal, M., and Bard, M. (1989). The yeast gene *ERG6* is required for normal membrane function but is not essential for biosynthesis of the cell-cycle-sparking sterol. Mol. Cell. Biol. **9,** 3447–3456.

Gachotte, D., Meens, R., and Benveniste, P. (1995). An Arabidopsis mutant deficient in sterol biosynthesis: Heterologous complementation by *ERG3* encoding a delta 7-sterol-C-5-desaturase from yeast. Plant J. **8,** 407–416.

Geng, Y., Whoriskey, W., Park, M.Y., Bronson, R.T., Medema, R.H., Li, T., Weinberg, R.A., and Sicinski, P. (1999). Rescue of cyclin D deficiency by knockin cyclin E. Cell **97,** 767–777.

Grebenok, R.J., Galbraith, D.W., and Penna, D.D. (1997). Characterization of *Zea mays* endosperm C-24 sterol methyltransferase: One of two types of sterol methyltransferase in higher plants. Plant Mol. Biol. **34,** 891–896.

Guo, D.-A., Venkatramesh, M., and Nes, W.D. (1995). Developmental regulation of sterol biosynthesis in *Zea mays*. Lipids **30,** 203–219.

Guthrie, C., and Fink, G.R. (1991). Guide to Yeast Genetics and Molecular Biology. (San Diego, CA: Academic Press).

Hajdukiewicz, P., Svab, Z., and Maliga, P. (1994). The small, versatile pPZP family of Agrobacterium binary vectors for plant transformation. Plant Mol. Biol. **25,** 989–994.

Hardwick, K.G., and Pelham, H.R. (1994). *SED6* is identical to *ERG6*, and encodes a putative methyltransferase required for ergosterol synthesis. Yeast **10,** 265–269.

Hartmann, M.-A. (1998). Plant sterols and the membrane environment. Trends Plant Sci. **3,** 170–175.

Husselstein, T., Gachotte, D., Desprez, T., Bard, M., and Benveniste, P. (1996). Transformation of *Saccharomyces cerevisiae* with a cDNA encoding a sterol C-methyltransferase from *Arabidopsis thaliana* results in the synthesis of 24-ethyl sterols. FEBS Lett. **381,** 87–92.

James, D.W., Jr., Lim, E., Keller, J., Plooy, I., Ralston, E., and Dooner, H.K. (1995). Directed tagging of the Arabidopsis *FATTY ACID ELONGATION1* (*FAE1*) gene with the maize transposon activator. Plant Cell **7,** 309–319.

Jefferson, R.A., Kavanagh, T.A., and Bevan, M.W. (1987). GUS fusions: β-Glucuronidase as a sensitive and versatile gene fusion marker in higher plants. EMBO J. **6,** 3901–3907.

Jensen-Pergakes, K.L., Kennedy, M.A., Lees, N.D., Barbuch, R., Koegel, C., and Bard, M. (1998). Sequencing, disruption, and characterization of the *Candida albicans* sterol methyltransferase (*ERG6*) gene: Drug susceptibility studies in *erg6* mutants. Antimicrob. Agents Chemother. **42,** 1160–1167.

Kauschmann, A., Jessop, A., Koncz, C., Szekeres, M., Willmitzer, L., and Altmann, T. (1996). Genetic evidence for an essential role of brassinosteroids in plant development. Plant J. **9,** 701–713.

Klahre, U., Noguchi, T., Fujioka, S., Takatsuto, S., Yokota, T., Nomura, T., Yoshida, S., and Chua, N.H. (1998). The Arabidopsis *DIMINUTO/DWARF1* gene encodes a protein involved in steroid synthesis. Plant Cell **10,** 1677–1690.

Madhani, H.D., Styles, C.A., and Fink, G.R. (1997). MAP kinases with distinct inhibitory functions impart signaling specificity during yeast differentiation. Cell **91,** 673–684.

Molzahn, S.W., and Woods, R.A. (1972). Polyene resistance and the isolation of sterol mutants in *Saccharomyces cerevisiae*. J. Gen. Microbiol. **72,** 339–348.

Nes, W.R., and McKean, M.L. (1977). Biochemistry of Steroids and Other Isopentenoids. (Baltimore, MD: University Park Press).

Nes, W.D., Janssen, G.G., and Bergenstrahle, A. (1991). Structural requirements for transformation of substrates by the (*S*)-adenosyl-L-methionine:delta 24(25)-sterol methyl transferase. J. Biol. Chem. **266,** 15202–15212.

Nes, W.D., McCourt, B.S., Zhou, W.X., Ma, J., Marshall, J.A., Peek, L.A., and Brennan, M. (1998a). Overexpression, purification, and stereochemical studies of the recombinant (*S*)-adenosyl-L-methionine:delta 24(25)- to delta 24(28)-sterol methyl transferase enzyme from *Saccharomyces cerevisiae*. Arch. Biochem. Biophys. **353,** 297–311.

Nes, W.D., He, L., and Mangla, A.T. (1998b). 4,4,14 Alpha-trimethyl 9 beta, 19-cyclo-5 alpha-26-homocholesta-24,26-dien-3 beta-ol: A potent mechanism-based inactivator of delta 24(25)- to delta 25(27)-sterol methyl transferase. Bioorg. Med. Chem. Lett. **8,** 3449–3452.

Nes, W.D., McCourt, B.S., Marshall, J.A., Ma, J., Dennis, A.L., Lopez, M., Li, H., and He, L. (1999). Site-directed mutagenesis of the sterol methyl transferase active site from *Saccharomyces cerevisiae* results in formation of novel 24-ethyl sterols. J. Org. Chem. **64,** 1535–1542.

Parish, E.J., and Nes, W.D. (1997). Biochemistry and Function of Sterols. (Boca Raton, FL: CRC Press).

Parks, L.W. (1958). *S*-Adenosylmethionine and ergosterol synthesis. J. Am. Chem. Soc. **80,** 2023–2024.

Prendergast, J.A., Singer, R.A., Rowley, N., Rowley, A., Johnston, G.C., Danos, M., Kennedy, B., and Gaber, R.F. (1995). Mutations sensitizing yeast cells to the start inhibitor nalidixic acid. Yeast **11,** 537–547.

Rahier, A., Taton, M., Bouvier-Nave, P., Schmitt, P., Benveniste, P., Schuber, F., Narula, A.S., Cattel, L., Anding, C., and Place, P. (1986). Design of high energy intermediate analogues to study sterol biosynthesis in higher plants. Lipids **21,** 52–62.

Schaller, H., Bouvier-Nave, P., and Benveniste, P. (1998). Overexpression of an Arabidopsis cDNA encoding a sterol-C24(1)-methyltransferase in tobacco modifies the ratio of 24-methyl cholesterol to sitosterol and is associated with growth reduction. Plant Physiol. **118,** 461–469.

Shah, N., and Klausner, R.D. (1993). Brefeldin A reversibly inhibits secretion in *Saccharomyces cerevisiae*. J. Biol. Chem. **268,** 5345–5348.

Shi, J., Gonzales, R.A., and Bhattacharyya, M.K. (1996). Identification and characterization of an *S*-adenosyl-L-methionine:delta 24-sterol-C-methyltransferase cDNA from soybean. J. Biol. Chem. **271,** 9384–9389.

Tong, Y., McCourt, B.S., Guo, D.-A., Mangla, A.T., Zhou, W.-X., Jenkins, M.D., Zhou, W., Lopez, M., and Nes, W.D. (1997). Stereochemical features of C-methylations on the path to 24(28)-methylene and 24(28)-ethylidene sterols: Studies on the recombinant phytosterol methyl transferase from *Arabidopsis thaliana*. Tetrahedron Lett. **38,** 6115–6118.

Welihinda, A.A., Beavis, A.D., and Trumbly, R.J. (1994). Mutations in *LIS1* (*ERG6*) gene confer increased sodium and lithium uptake in *Saccharomyces cerevisiae*. Biochim. Biophys. Acta **1193,** 107–117.